Supporting Information

Strongly Enhanced Cooperative Surface Propensity of Atmospherically Relevant Organic Molecular Ions in Aqueous Solution

Harmanjot Kaur, Stephan Thürmer, Shirin Gholami, Bruno Credidio, Florian Trinter, Debora Vasconcelos, Ricardo Marinho, Joel Pinheiro, Hendrik Bluhm, Arnaldo Naves de Brito, Gunnar Öhrwall, Bernd Winter, and Olle Björneholm

Accounting for signal saturation and sample contamination

Two experimental issues were encountered during the measurement in a few cases: photoelectron (PE) signal saturation and additional contaminants' signals. Both effects could be mitigated, as explained in the following with the help of Figure SI-1.

As explained in the main text, in some cases the C 1s PE signal intensity was underestimated and became so high as to saturate the detector, which occurred at about 2000 counts per second (cps) per channel or ~2 x 10^5 cps integrated. This affected four out of the 24 solutions used, with the most severe case presented in Figure SI-1A. This issue was recognized during the experiment and measurements at a lower-photon-flux setting were performed; here, the beam-defining aperture (BDA) of the beamline was closed to about 1/3 to 1/4 of the usual setting; the low-flux example in the figure was measured at an aperture setting of 1.4 mm versus 6 mm for the high-flux case. For 400 eV photon energy, we used BDA settings of 6 mm, 2 mm, 1.75 mm, 1.6 mm and 1.4 mm corresponding to photon fluxes (in units of 10^{12} photons/s) of 7.1, 3.1, 2.4, 2.0, and 1.2, respectively. For 510 eV photon energy, we used BDA settings of 6 mm, 2 mm, 1.75 mm, 1.6 mm, and 1.35 mm corresponding to photon fluxes (again in 10^{12} photons/s) of 9.5, 4.0, 3.2, 2.6, and 1.4, respectively. The resulting low-flux spectrum is free of saturation effects while still having a sufficient signal-to-noise ratio and was used for further analysis. A scaling factor was employed to compensate for the reduced flux. Here, we did not rely on the photon-flux values for normalization, since alignment and other experimental details can additionally alter the count rate. Instead, we used the measured spectra directly for comparison. Since the C 1s peak of the functional group (at low KEs to the left) is always below the saturation limit, it could be used as a reference for scaling the low-flux to the high-flux results. The determined scaling factor (5.975 in the example of Figure SI-1) was then applied to all extracted intensity values.

Figure SI-1B shows an exemplary fit to the C 1s PE spectrum of aqueous formate (C1). Instead of only one feature corresponding to the sole C site of the molecule, additional weak features appear, which are considered contaminants of unknown origin. Whenever such additional features were identified in the spectra, they were fitted with additional Gaussians, but omitted from the reported peak intensity values. There is a possibility that the results of the mixed species are somewhat affected by these contaminants, but since the contaminant signal is small, we consider them negligible for the overall result. Furthermore, considering that these contaminants are unlikely to be surface-active, they thus play a diminishingly small role for the results of highly surface-active species.

Analysis of the valence-band PE signal as a function of solute species and concentration

Figure SI-2 shows the valence-band PE spectra for the single-species aqueous solutions. Here, the valence-band signal of each solution was scaled so that the intensity of the liquid-water $1b_1$ band of each solution matched that of an average neat-water spectrum. The resulting scaling factors are an indication of the signal reduction of the solvent due to surface coverage by the solute. An average neat-water PE spectrum was used as a reference, chosen from repeated neat-water measurements during the experimental campaign. Fluctuations in the neat-water intensity were on the order of ±0.02 around the average.

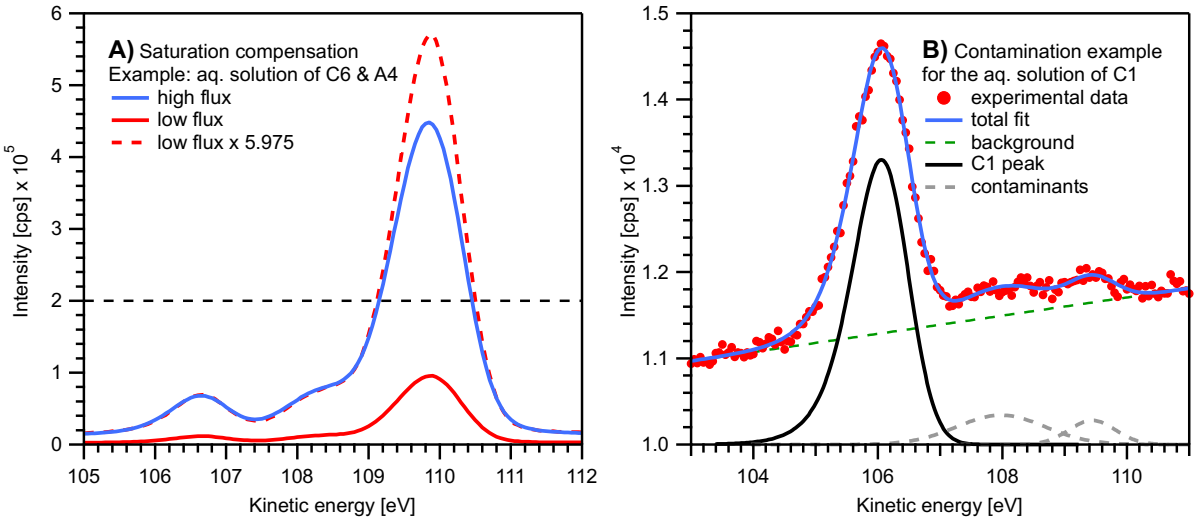

Figure SI-1: Treatment of experimental issues: **(A)** signal saturation and **(B)** contaminant signals.

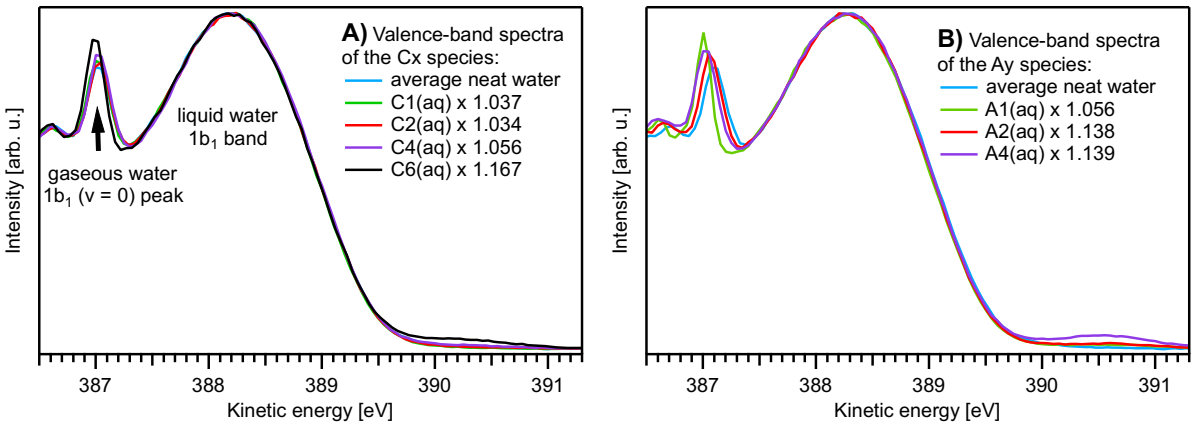

Figure SI-2: Analysis of valence-band intensity for single-species aqueous solutions: **(A)** Cx(aq) and **(B)** Ay(aq); A6 is not shown as this species was measured in a different experimental campaign. Each solution's PE spectrum was scaled until the intensity of the liquid-water $1b_1$ band matched that of an average neat-water spectrum. Scaling factors to achieve this are indicated in the legend.

The resulting reduction in signal (inverse of the scaling factor) is plotted against the number of carbons within the solute molecule in Figure SI-3. A downward trend is observed for both species. Since the solution–vapor interface is successively covered more and more by solute molecules with increased surface propensity, photoelectrons from the solvent experience more and more inelastic scattering with the solute, which reduces the average PE signal intensity in the direction of the detector. Thus, the valence-band signal reduction confirms our observation of an increased surface coverage. While the effect is small and depends strongly on the surface coverage and orientation by the solute molecules, a significant decrease is

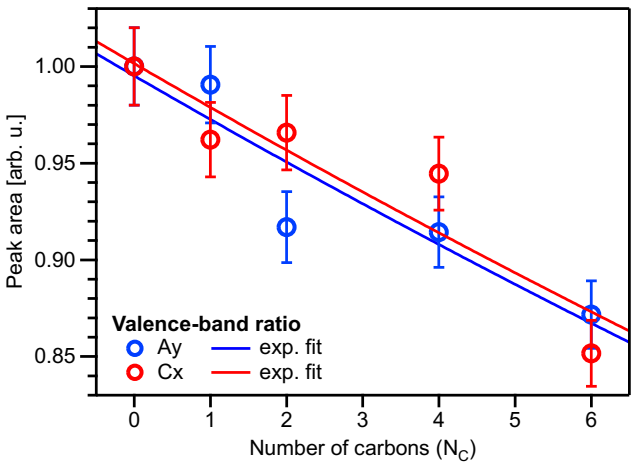

Figure SI-3: Valence-band ($1b_1$) PE intensity relative to neat water (= 1) for aqueous solutions of the Cx (red circles) and the Ay (blue circles) species, respectively.

observed. The strongest reduction of the valence-band intensity is observed for C6 and A6, for which the intensity is ~86% of the intensity for pure water. We can use this to estimate the amount of organics on the surface by approximating it with a compact layer. With an EAL of 15 Å, this corresponds to a layer thickness of ~2.2 Å. Note that we find already a reduction in intensity for the smallest species C1, which we have designated as not surface active in the main text. This result is, however, still within error bars of the neat-water case, but shows that reality may deviate somewhat from our assumption of zero surface propensity for C1. This is expected, as equilibrium dynamics driven by Brownian motion are bound to push at least some molecules to the surface even in the case of hydrophilic species.

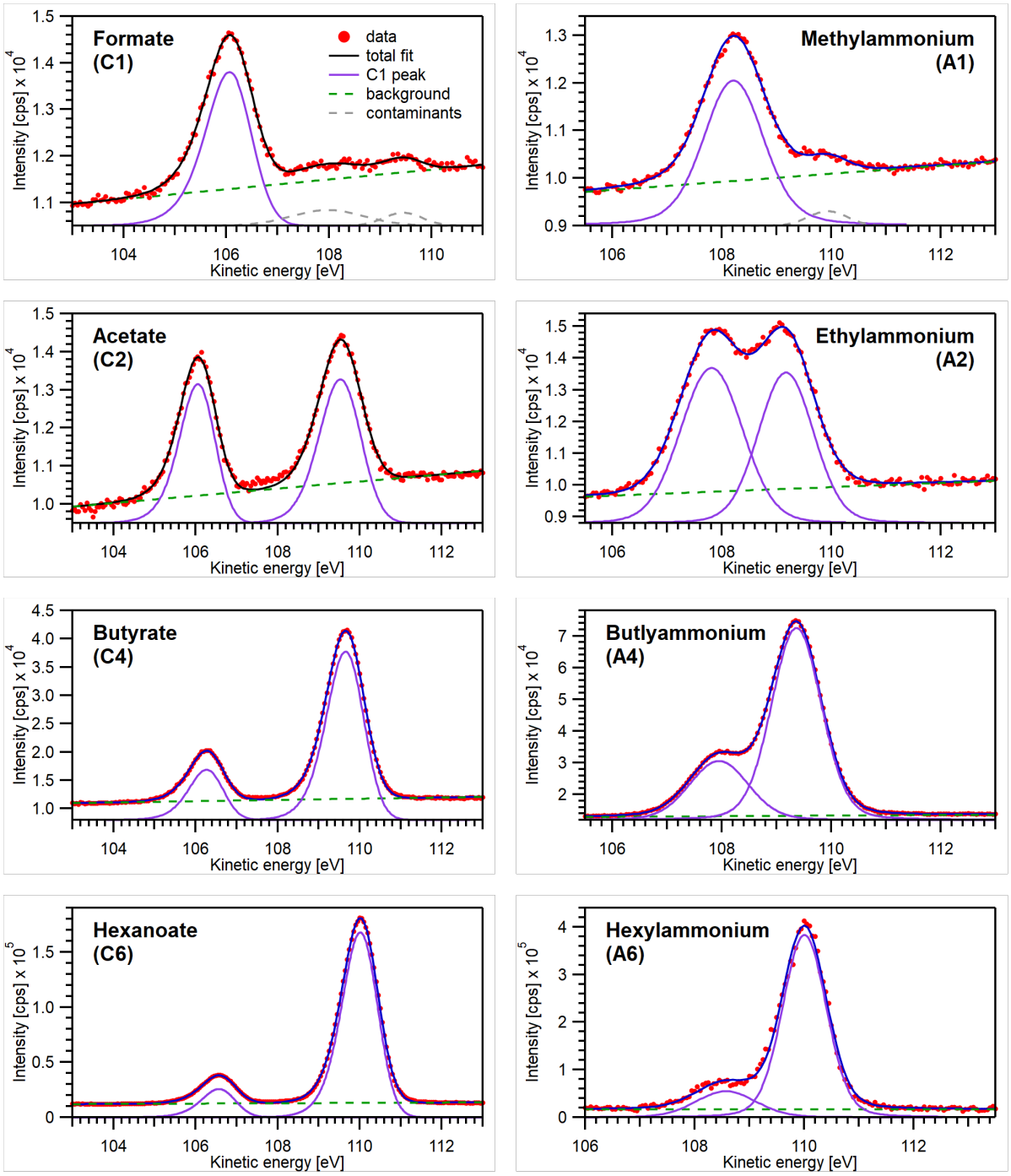

Figure SI-4: PE spectra (red dots) of the single-component solutions together with the total fits (black) and individual peak components (purple). Dashed grey lines indicate contributions from contaminants and green dashed lines are the linear background. Intensities of the C6 and A6 spectra are scaled to account for the different BDA slit setting for the former and the overall intensity difference due to experimental settings for the latter.

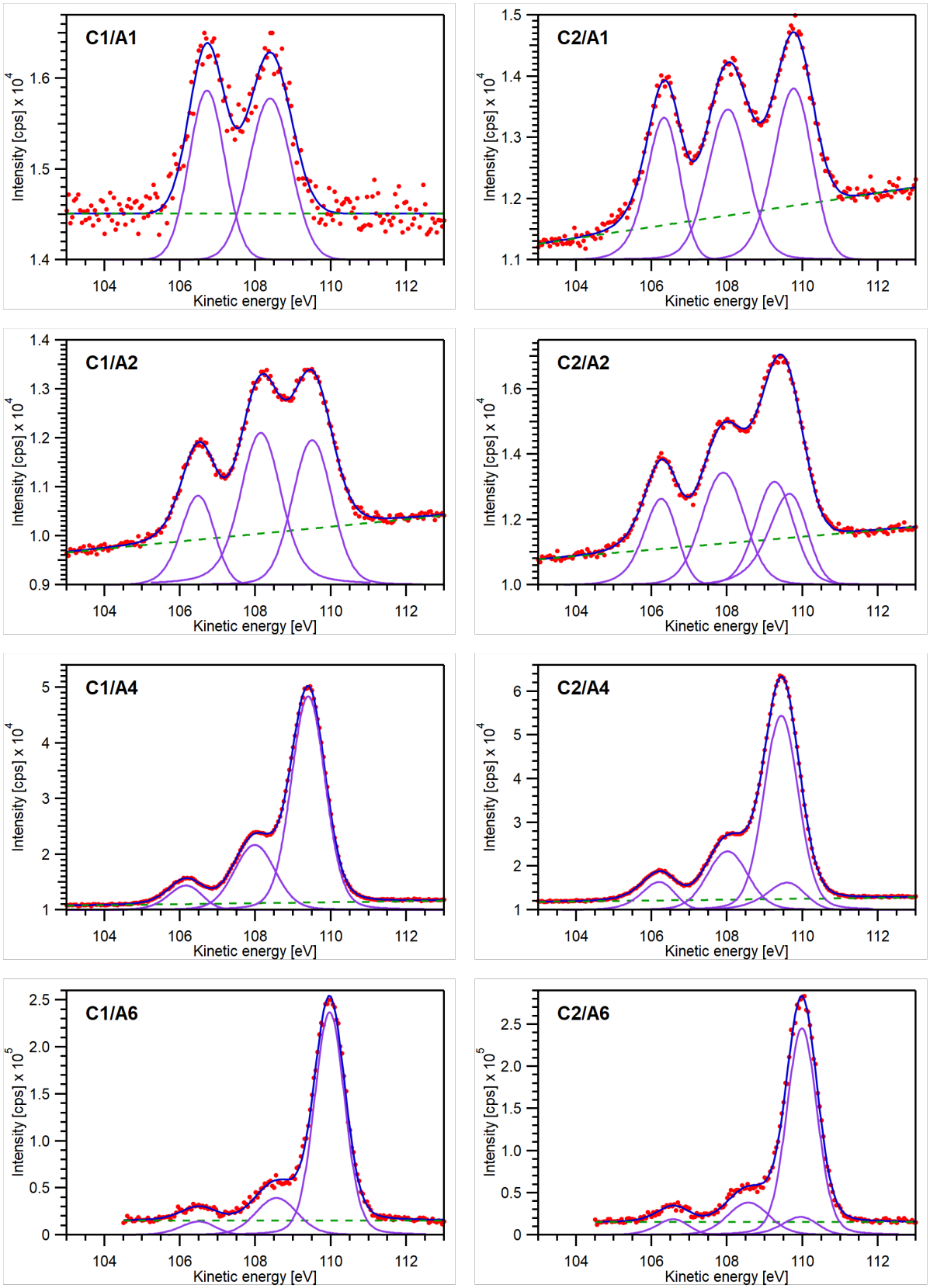

Figure SI-5: PE spectra (red dots) of the mixed-component solutions Cx/Ay (x = 1,2 and y = 1,2,4,6) together with the total fits (black), individual peak components (purple), and the linear background (green dashed line). Intensities of the spectra for the C1/A1, C1/A6, and C2/A6 mixtures are from a different measurement campaign. These spectra are scaled according to a factor to match a reference measurement of C1 in each campaign.

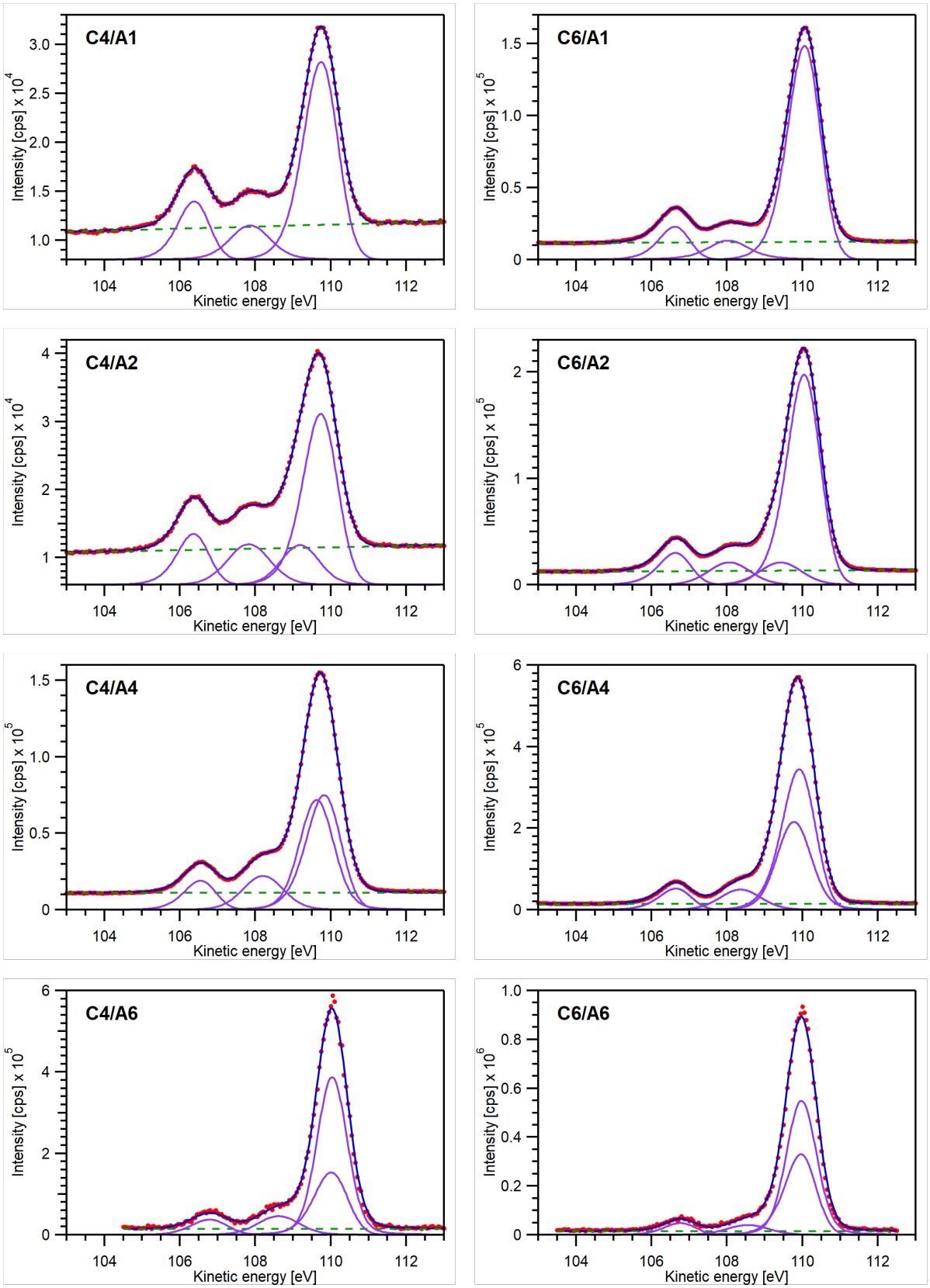

Figure SI-6: PE spectra (red dots) of the mixed-component solutions Cx/Ay (x = 4,6 and y = 1,2,4,6) together with the total fits (black), individual peak components (purple), and the linear background (green dashed line). Intensities of the spectra for the C4/A6 and C6/A6 mixtures are from a different measurement campaign. These spectra are scaled according to a factor to match a reference measurement of C1 in each campaign.